Realization of GHz band integrated optical links in a radio frequency Si Ge bipolar process operating at 650 to 850 nm wavelength

Lukas W Snyman, Kingsley A Ogudo, Zerihun G Tegnege, Anne-Laure Billabert, Herzl Aharoni, Jean-Luc Polleux

Realization of GHz band integrated optical links in a radio frequency Si Ge bipolar process operating at 650 to 850 nm wavelength

Lukas W. Snyman,[a,*] **Kingsley A. Ogudo**,[b,c] **Zerihun G. Tegnege**,[c] **Jean-Luc Polleux**,[c] **Anne-Laure Billabert**,[d] **and Herzl Aharoni**[e]

[a]University of South Africa, Institute for Nanotechnology and Water Sustainability Research, Pretoria, South Africa

[b]University of Johannesburg, Department of Electrical and Electronics Engineering Technology, Johannesburg, South Africa

[c]Université Paris-Est, ESYCOM-CNRS, ESIEE Paris, Le Cnam, UPEM, Cite Descartes, Noi-sy-Le-Grand-Cedex, France

[d]Université Gustave Eiffel, ESYCOM-CNRS, Le Cnam, Paris, France

[e]Ben Gurion University of the Negev, Be'er Sheva, Israel

Abstract. A series of on-chip optical links of 50-μm length, utilizing 650 to 850 nm propagation wavelength, with Si avalanche-mode optical sources, silicon nitride-based waveguides, and Si Ge detectors, have been designed and realized, with a 0.35-μm SiGe radio frequency bipolar integrated circuit process. The optical coupling between the optical source and the detectors was realized by a set of dedicated designed optical waveguides, which were all fabricated with components of the SiGe radio frequency process. All components were fully integrated on the same silicon chip. The Si avalanche-mode light-emitting diodes (Si AMLEDs) emitted in the 650- to 850-nm wavelength regime. Correspondingly, small microdimensioned detectors utilize SiGe detector technology with detection efficiencies of up to 0.85 in the same wavelength regime and with a transition frequency of up to 20 GHz. Best performances for the optical links as realized show optical coupling of up to 5 GHz with a total optical link budget loss of −40 dB. A set of link results are presented and several interpretations are given on current realizations. The technology is particularly suitable for realization of low-cost on-chip optical signal processing, optical interconnects, and various types of on-chip microsensors. [DOI: 10.1117/1.OE.61.12.125109]

Keywords: electroluminescence; light emitting diodes; silicon; silicon integrated circuitry; optical wave-guiding; optical detectors; optical communication.

Paper 20220880G received Aug. 14, 2022; accepted for publication Nov. 30, 2022; published online Dec. 28, 2022.

1 Introduction

Various researchers in integrated optoelectronics have highlighted the need for small-dimension optical communication systems, which can be integrated into mainstream silicon fabrication technology and particularly in complementary metal oxide semiconductors (CMOS) technology and silicon Bi-CMOS technology.[1–6]

The on-chip optical coupling structures may replace the parallel metallic bus-based coupling usually used for signal transmission between devices, facilitating higher rate of signal processing. Particularly, the monolithic integration of SiLEDs, on-chip silicon-based waveguides, and on-chip silicon detectors would offer low-cost communication, signal processing, all integrated onto the same chip and utilizing adjacently lying analog and digital interfacing technology. The low-cost aspects, submicron dimensioned processing, and on board integrated electronic processing as offered by silicon mainstream bipolar and CMOS-based silicon technologies, offer various advantages in terms of production costs and ease of manufacturing, even if systems and

*Address all correspondence to Lukas W. Snyman, snymalw@unisa.ac.za

components do not compete with high-end, more complex, and more complex technologies. Si avalanche mode light-emitting diodes (Si AMLEDs) that emit in the 450- to 750-nm regime have been known since the 1950s.[7,8] A particular pioneering revisit of the Si AMLEDs in n + p guard ring protected structures, and that ensured more uniform planar emissions, was demonstrated in the early 1990s.[9,10] Si AMLEDs that are completely compatible with mainstream CMOS integrated circuit technology, however, only emerged in the 1990s.[11–15]

In the early 2000s, optical links operating at 1550 nm wavelength have been realized in the end process regime of a CMOS process, after completing all the high-temperature rapid thermal annealing activation of CMOS implants.[16–18] However, realization of practical and efficient optical sources as well as detectors at 1550 nm offered substantial challenges.

Since 2000, our group has realized first iteration of all-silicon and CMOS on-chip optical links, for operation in the 450- to 850-nm wavelength regime, utilizing an Si AMLED source, a $5 \times 1 \times 150$ μm silicon nitride over layer waveguide and a specially designed, lateral incident optimized, CMOS-based photodetector.[17,19,20] Operation at this wavelength would enable integration of both optical source, waveguides, and detectors in this mainstream technology at low-cost factors and possible widescale new applications. This would enable the realization of an optocoupling system monolithically on the same chip using mainstream silicon fabrication technology. We particularly endeavor design and realization of waveguiding structures, such that the optical radiation can be transported some distance on the chip between the optical source and the optical detector. Because of the low-cost manufacturing possibilities, relative simplicity in the process, we believe that many applications may arise in future. Propagation of the optical radiation in the silicon overlayers and leakage of the propagated light from bends in the waveguide; however, it seemed challenging at the time.

Recently, Xu et al.[21] introduced MOSFET gated modulation Si AMLEDs, which can in simulation be modulated to 10 GHz plus.

Dutta et al.[22] and Agarwal et al.[23] recently presented optical coupling in a monolithic laterally coupled wide-spectrum ($350\ \text{nm} < \lambda < 1270\ \text{nm}$), optical link in a silicon-on-insulator CMOS technology. The link consists of a silicon (Si) light-emitting diode (LED) as the optical source and a Si photodiode (PD) as the detector; both realized by vertical abrupt n + p junctions, separated by a shallow trench isolation composed of silicon dioxide. Medium trench isolation around the devices along with the buried oxide layer provides galvanic isolation. Optical coupling in both avalanche-mode and forward-mode operation of the LED is analyzed for various designs and bias conditions. The novelty of this work is the use of highly sensitive single-photon avalanche diodes for photodetection to compensate for the low internal quantum efficiency of SiAMLEDs. They investigated their optocoupler realized in a standard 140-nm CMOS SOI technology, without postprocessing, for various LED designs and points of operation. The power consumption of the AMLEDs was minimized through a design and employment of a low-power LED driver circuit. For the best AMLED design, the achievable data rate was a few Mbps and the energy consumption a few nJ/bit. The active area of the proposed systems is $<0.01\ \text{mm}^2$ over a distance of 50 microns.[23–25]

Recently, our group has realized a new set of optical sources, three different waveguides, and a new set of SiGe detectors for operation in 450 to 850 nm wavelength, which could boost the responsivity as well as the upper frequency and cut-off frequency of such links.[26,27] We utilized a combination of high-speed SiAMLED sources, Si nitride waveguide technology, and high-speed Si-Ge detector technology to achieve this goal. An overview paper of our achievements with regards to realizing first iteration complete optical link structures operating utilizing Si Ge bipolar technology in the 450- to 850-nm band was published in SPIE Optical Proceedings of 2014.[28] We, in overview, highlighted the design of the optical link structures, utilizing the SiGe 0.35-μm processing technology. However, we observed high losses, presumably caused by means of weak aligning of optical source to waveguide and from waveguide to detector structures.

In this paper, more detail about our design strategies with regard to realization of optical links in a SiGe 0.35-μm bipolar radio frequency (RF) process is given. Several new results are presented, especially for the vertical pillar like structures, as previously reported in Ref. 28. Particularly, we present more detail about the direct current (DC) and RF coupling results that have been observed for the structures. We analyze the various resistive and capacitive parasitic coupling effects that occur in the overlayers and also through the substrate, itself. Finally, we highlight potential high-impact applications for these Si AMLED-based optical links.

2 Design Strategies as Implemented in Our Latest Optical Link Designs

The optical wave guiding characteristics as associated with our optical sources and detector structures as implemented in our optical links have recently been reported extensively in Refs. 12,13,29. Only the major design aspects of the Si AMLED Technology with the 0.35-μm SiGe RF process technology and design detail of the latest silicon oxide and nitride-based optical waveguides are reviewed here.

2.1 *Utilization of Si AMLEDs as Optical Sources in the Optical Links*

Si AMLEDs offer the following advantageous for integration into Si mainstream technology.

1. They can emit up to 10 to 100 nW/μm^2 at 450 to 750 nm regime at compatible CMOS operating voltages and currents levels (3 to 8 V and 0.1 to 5 mA).[30–32]
2. The emission levels of the Si CMOS AM LEDs are 10^{+3} to 10^{+4} higher than the detectivity of silicon p–i–n detectors and hence offer good dynamic range in detection and analyses.[33–35]
3. Very high modulation speed possibilities (>10 GHz) with direct driving as well as MOS gate circuit modulation of the sources.[36]
4. They can be incorporated at the silicon–SiO_2 interface level since they are high-temperature processing compatible. The emission wavelength can be reasonably engineered from very broadband to quite narrow band emissions by incorporating specific wavelength engineering processing procedures. Particularly, p + n designs show strong spectral emissions around 0.75 μm.

Recently, particularly, promising results have been obtained through introducing injection of additional carriers into avalanching junctions,[37] and depletion layer profiling and applying dedicated carrier and momentum engineering.[38,39]

2.3 *Developing Silicon Nitride-Based Optical Waveguides in Silicon RF 0.3 Bipolar Technology*

Our optical waveguide design, take advantage of the different oxide layers of the Si-Ge 0.35 bipolar technology as outlined in Sec. 2.1. Detail results have already been given about our waveguide design strategies and corresponding simulation results. Only a brief review is hence presented here.[27,28]

Figure 1 shows some conceptual aspects of our latest waveguide design strategies, utilizing the 0.35-μm Si Ge RF bipolar process. In a first design (waveguide design 1), as in Fig. 1(a), the waveguide structure was placed in the outer overlayers of the plasma deposit layers. These consisted mainly of tetra-ethoxy silane (TEOS) overlayers of $n = 1.46$ and then filled with a second TEOS layer (darker yellow in this figure), as densified by thermal process, increasing its refractive index to about 1.48. A V-shaped cross-section as defined by built-in processing procedures ("bonding pad" definition) was used to ensure etching of crevices down to the silicon substrate level. This confined lateral waveguiding of the propagated light, while vertical confinement of the propagated light was ensured by the difference in the refractive index vertically in the center TEOS layers. The optical source was slightly subsurface of the top layer of the pillar structure and good optical coupling were presumably facilitated by light radiating spherically from the source and coupling both laterally and vertically into the waveguide.

In a second design (waveguide design 2) as in Fig. 1(b), an etched crevice of 0.4 μm in the first TEOS layer was filled up with a silicon nitride over layer, using the "capacitor" definition of the RF 0.35 μm RF process, followed by further CVD deposited TEOS oxide over layers. Hence a high refractive index core of $n = 2.4$ were formed with a surrounding index of $n = 1.46$.

In a third design, as in Fig. 1(c) (waveguide design 3), the lateral width of the silicon nitride layer was reduced to 0.3 μm in order to form a narrow higher index core, which would enable a less multimode propagation and lower optical dispersion of the optical radiation from the source.

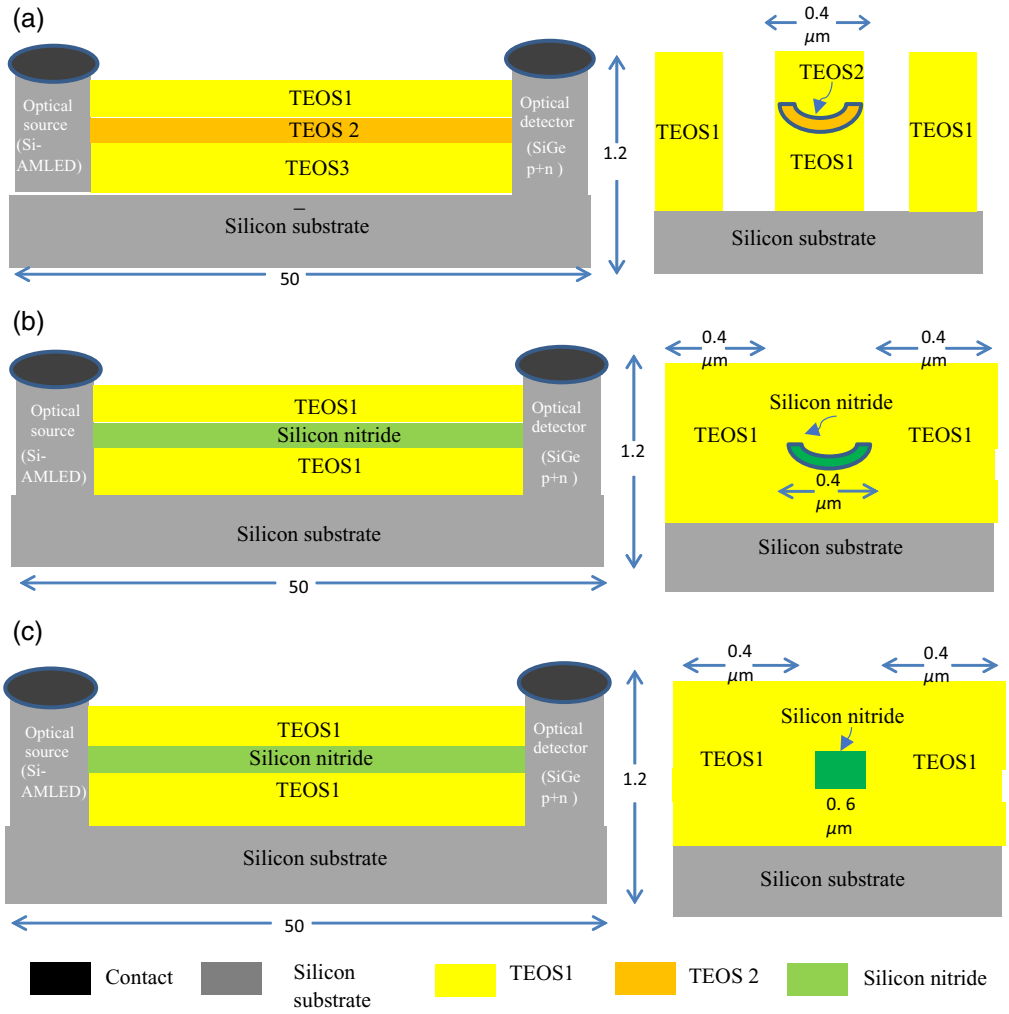

Fig. 1 Schematic presentations showing the three basic designs (a) OLTS1, (b) OLTS2, and (c) OLTS3 of waveguides as implemented in this study. All dimensions are given in μm. A lateral and cross-sectional layout is presented in each case.

At the shorter wavelengths, silicon nitride reveals higher absorption coefficients.[40] Simulation results for waveguide design 1, as in Fig. 1(a), at 650 nm revealed broader propagation with some loss in the beginning of the waveguide near to the source position.[27] Simulation results reveals a narrower core waveguide narrower propagation, with very low loss and with a multimode propagation. Multimode propagation has the advantage of allowing both a large acceptance angle for coupling of the optical radiation from the silicon LED into the waveguide as well as for emission of light out of the waveguide at the end of the waveguide, and they can also accommodate high curvatures in the waveguides. With waveguide design 3, a single-mode propagation prediction was indeed achieved. Although much more difficult to couple light into the smaller core, we see lower modal dispersion loss along the waveguide. This design hence enables extreme high modulation bandwidths to be achieved in the waveguides with dispersion of 0.5 ps cm^{-1} and a bandwidth-length product of a value higher than 100 GHz cm for a 0.2-μm silicon nitride-based core. A maximum modal dispersion of 0.2 ps cm^{-1} and a bandwidth-length product of higher than 200 GHz cm for a 0.2-μm are observed for this design.

3 Realization of Complete On-Chip Optical Link Structures in a 0.35-μm Si Ge RF Bipolar Process

The whole optical link structure was realized on the silicon substrate of very high resistivity (500 MΩ cm). Channel doping layers were used to contact bottom layers of the detectors, and

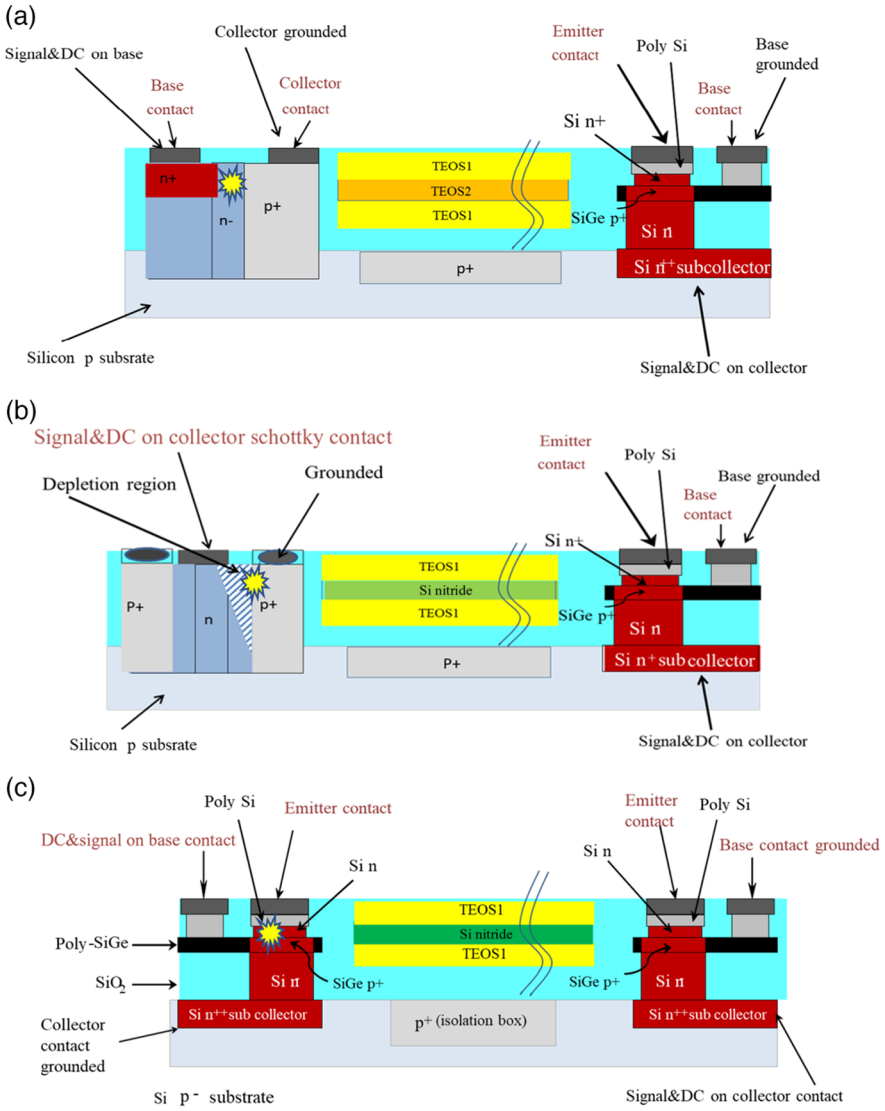

Fig. 2 More detailed design layouts of the three different optical link structures, showing the different building blocks of the structures using the 0.35-μm Si Ge Bi CMOS process. (a)–(c) OLTS1 to OLTS3. The SiAMLED emission points in the structures are correspondingly indicated.

micron-dimensioned metal contacts were used to access topmost device regions, including the Ge-based-doped layers used in the Si-Ge phototransistor designs (as were illustrated in Fig. 1). Typical doping, resistivity, and dielectric coefficients of the respective oxide layers were numerically calculated. The resistances of the respective components were, such as the isolation p+ channel stop implant region resistance and p+ reduce substrate resistance.[25] Three different optical link structures were realized in these analyses and subsequently analyzed in terms of forward transmission parameters, reverse scattering parameters, and gain between the optical source and the detector.

In a first test structure 1 (TS1), as shown in Fig. 2(a), an n–p–n columnar structure was designed as a optical source structure that was arranged laterally on the semi-insulating substrate, and perpendicular to the propagating direction. A similar structure was used to realize the integrated phototransistor structure with a Ge-doped base. The columnar structures were all of micron dimension, such that the structures were composed of about 1 μm cube substructures. The various regions were doped as indicated. The regions were appropriately electrically contacted during experimental measurements to reverse bias the first p^+n junction. Upon reverse biasing, the depletion region penetrates through to the n+ region in order to strengthen and unified the electric field in the lowly doped n region. From our previous device designed experience,

we established that the light emission would occur at the p^+n interface near the surface region, and with increase in voltage bias, extend over the middle n region toward the second np+ junction. The region between the Si Av LED source and SiGe detector was filled with normal TEOS plasma deposited oxide as part of the available process procedure.

This specific design included positioning of several different thicknesses of TEOS layers, as in waveguide design 1, in Fig. 1(a), with air side slots and a densified middle TEOS layer. The purpose of the design was to place components such that light as emitted from the optical source were aligned optimally such that light could couple effectively into the higher indexed layer and that light would then be propagated along the waveguide over some 50 μm toward the detector structure. In the real structure, the source lateral structure was in fact orientated 90 deg with respect to the inlet of the waveguide structure. A SiGe heterojunction bipolar transistor (HBT) was selected with a width of 5 μm and a length of 1.2 μm. The base–collector regions were reversed biased to separate the photogenerated electron–hole pairs. The base emitter structure was short-circuited with a 50-Ω load resistor to operate in the PD mode to simplify initial detector measurements and to maximize the operating bandwidth, at the expense of reduced responsivity.

In a second test structure 2 (TS2) as in Fig. 2(b), the same basic lateral columnar structure was used, but a rectangular Schottky contact of aluminum on n-silicon was fabricated in the columnar structure middle lowly doped n region. The two p+ columnar regions were grounded as required by the RF probe bias and measurement process, and the modulation signal was applied on the Schottky contact. Positive voltage bias placed the Schottky contact in forward bias mode making it ohmic in conduction. Reverse biasing the p+ n region at the one column side, a triangular depletion region would form and extend toward the p+ region. This configuration reduced the total depletion region volume and hence reduces the total depletion layer capacitance as compared with the previous design. The elongated and uniform electric field region, and its associated minimized capacitance, would enable higher modulation frequencies of the Si avalanche mode optical LED source. Since small dimensions were used and the light emission processes are impact ionization and avalanche related, calculations showed that modulation frequency of up to 300 GHz could potentially be reached. A V-shaped groove waveguide design waveguide design 2 as in Fig. 1(b) was used, in order to optimize coupling of light from a circular and spherical nature and to improve optical coupling with the micron dimensioned emissions from the Si Av LED. The same detector structure design was used as in TS1.

In a third test structure 3 (TS3) as in Fig. 1(c), a vertical cubical columnar structure was used for both the optical source as well as the detector. The Si-Ge-based region in the same volume structure was used for optical detection. Si-Ge pn junction (HBT emitter collector junction) was placed in reverse bias and biased into avalanche mode. Since the Si-Ge structure of this nature has a transition frequency of up to 80 GHz, it can be assumed that the reverse bias base–collector junction, when placed in avalanche reverse bias mode, could attain similar modulation The optical waveguide was similar as in TS2, but the silicon nitride layer lateral thickness was strategically reduced in lateral width dimension as in optical waveguide structure, design 3 as in Fig. 6(c). The purpose of this choice was to reduce the waveguide core size and enable less modal dispersion in the waveguide.

Figures 3(a)–3(c) show visual presentations of one of the complete optical link structures, OLTS3, as it appeared with normal illumination conditions under an optical microscope.

4 Experimental Results

4.1 *DC Bias Analysis*

DC bias and current analyses were performed on all three of the optical links test structures. The latest DC results as measured for TS1 to TS3 are presented in Fig. 4. Detector current responses were observed as shown in Fig. 4(b) when the source was reverse biased in avalanche mode as in Fig. 4(a). An observed nonresponse signal or "dark" current of the order of 10 to 20 nA was observed for all three test structures. When the bias voltage passed the knee activation voltage of each Si AMLED, and the avalanche and light emission processes

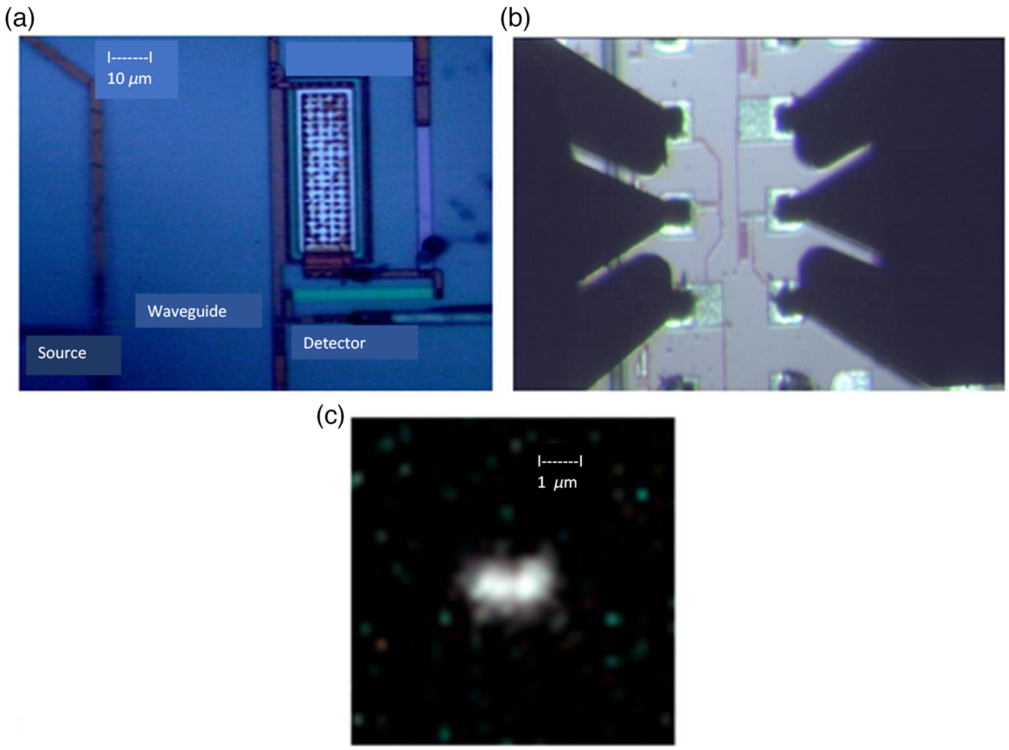

Fig. 3 (a) Bright field micrograph of the optical microlink device as realized in a 0.35-μm Si-Ge RF process technology; (b) micrograph of G-S-G bias probe on one of the device at measurement; and (c) a typical emission pattern as observed for our Si AMLED in OLTS 3.

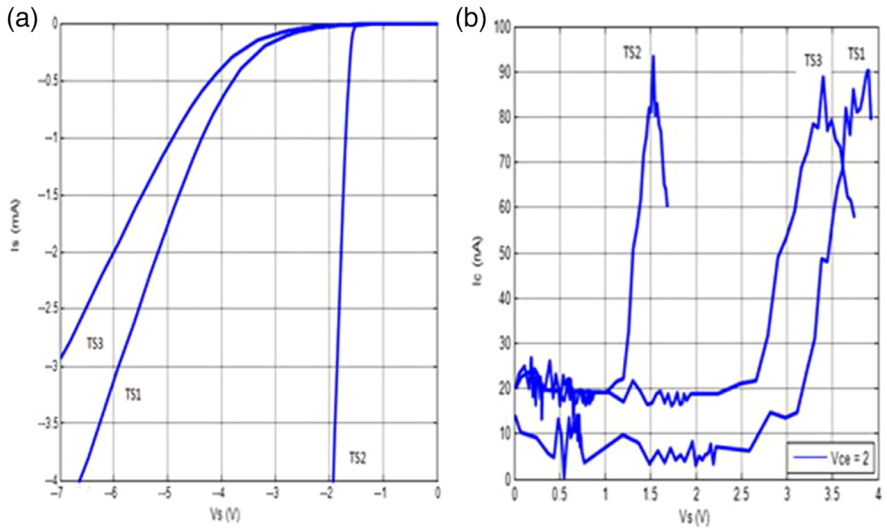

Fig. 4 (a) DC voltage and current bias curves and (b) detector response curves for TS1 to TS3 when source was activated as in (a).

were activated in each case, the respective detector currents increased to about 90 to 100 nA in each respective case. This observation indeed confirmed that optical propagation did occur from the optical sources to the waveguide structures. An analysis also showed that the magnitude of the detector currents and indicated that some waveguiding did occur in each case, since much lower responses would be detected if only spherical radiation occurred from each source.

4.2 *AC Coupling Analysis*

Figure 4(a) shows bright field micrograph of the optical microlink device as realized in a 0.35-μm Si-Ge RF process technology. Figure 4(b) shows the 200-μm pitch of type ACP40W ground-signal-ground probes as connected in one of the devices on the die with a HP model 8510 (50 MHz to 40 GHz) network analyzer during the experimental measurements. Where possible, both sides of the structure were grounded on the same ground, in order to ensure that no parasitic coupling effects would arise when biasing both the optical source and the detector.

Thorough forward transmission scattering S21 and reverse scattering parameters S12 and source S11 and detector scattering S22 were analyzed for each test structure, and with proper source and load matching circuitry implemented.

When optical propagation did occur from the source to the detector, the detector will generate additional detector current, which would impose a higher voltage into the matched load, and a subsequent higher forward transmittance S21. This would indicate that optical coupling did indeed occur between the optical source and the detector. Our theoretical calculations indicated that, if only spherical radiation occurred from the optical source, over a 50-μm distance isotopically radiated from the source, an about −60 dB loss would be expected. Any higher value observed for S21 in the structures would hence be indicative of optical coupling between the optical source and the detector. A high S12 scattering parameter, on the other hand, would indeed indicate that a feedback effect was observed at the source as a result of signal generated at the detector. This would indicate that some form of parasitic coupling effect did occur, either through the dielectric overlayers, or through the silicon substrate.

Figure 5 shows our latest RF coupling analyses for our realized optical link structures. Figure 5(a) shows the coupling parameters that were observed for TS1. It shows low and about equal values for both S21 and S12. A −50-dB coupling was observed for S21 between the source and the detector, particularly at the higher frequencies toward 5 to 10 GHz. A same magnitude coupling was observed for S12 in this structure. This indicated that some high parasitic coupling effects were observed in this optical link structure, either through the dielectric overlayers or through the silicon substrate itself. Hence the general conclusion for the results of this structure

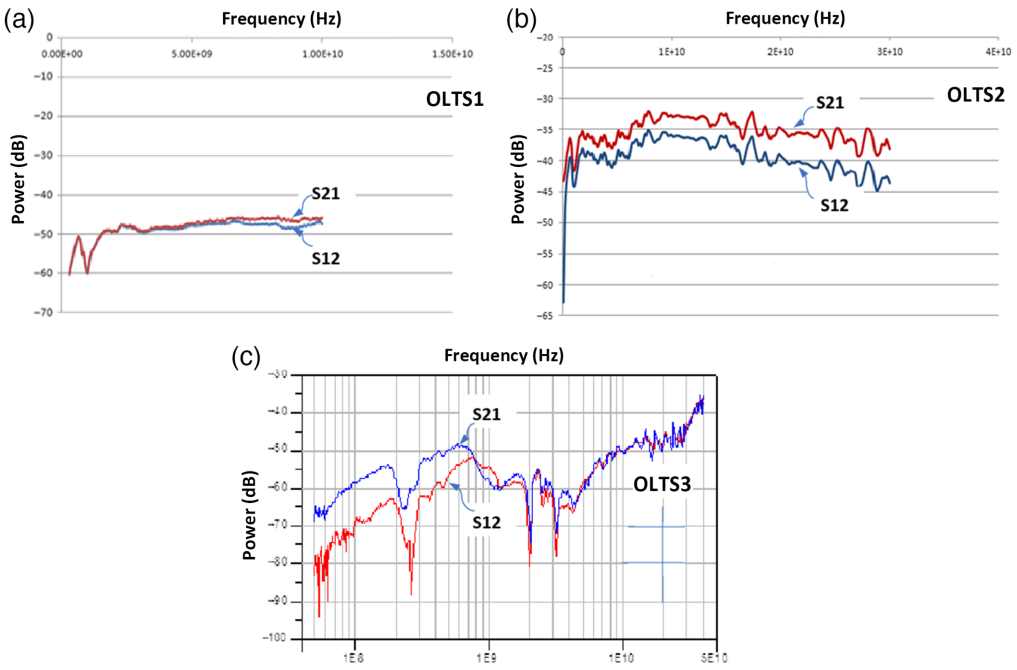

Fig. 5 Forward transmission scattering parameters as were observed for the three realized optical link structures with a Si Ge bipolar RF process, OLTS1, OLTS2, and OLTS3, in (a)–(c), respectively. Optical waveguide structures as in Figs. 2(a)–2(c) respectively. Especially, TS2 and TS3 reveal optical coupling to well into the GHz range.

was that there was indeed very low optical coupling occurring through the deposited TEOS oxide overlayers in this structure. Furthermore, a high parasitic RF coupling also occurred through this structure either through the overlayers or through the silicon substrate itself. However, further experimental investigations should be conducted.

Figure 5(b) shows results as observed for test structure TS2, with the Schottky contact reverses bias structure and with a silicon nitride core waveguide as in Fig. 2(b). A clear higher coupling value is indeed observed for S21 as compared with S12. According to our earlier interpretations as above, this clearly indicates that some optical propagation did occur along the waveguide. The Schottky contact in the source "pillar" structure [Fig. 2(b)] also presumable reduced both the parasitic resistance and the parasitic capacitance to ground between the source contact layers and the substrate itself as compared to the source structure in OLTS 1 in Fig. 2(a). Particularly, the depletion layer extended more along the surface layers and avalanche light processes occurred more confined at the second np+ junction, reducing the capacitive coupling to ground substantially, as compared to the structure and design in OLTS 1 in Fig. 2(a). This was indeed an important design consideration that was introduced during the design phases of this structure. Also, the optical source was probably better aligned with the waveguide, and hence a good optical coupling occurred through the waveguide. The −40-dB coupling for S21 indeed indicates about one-order higher optical coupling for this link structure. Also the forward transmission scattering parameter S21 is much higher that the reverse scattering parameter S12, further confirming that optical coupling did occur in the structure. The fact that higher S21 than S12 is observed up to about 2 GHz and beyond is indicative of the high modulation frequencies that can be achieved with these types of structures. The decay in S21 as a function of increase in frequency at higher frequencies is typical for parasitic coupling from the signal source to ground at higher frequencies. The most probable path would be the parasitic resistive path to ground between the Schottky contact and Si LED contact regions through the silicon pillar structures [Fig. 2(b)] and then along a path in the substrate to the detector along the silicon substrate itself.

Furthermore, the elongated surface electric field region as provided by the Schottky contact, and its associated minimized capacitance, seemingly enable higher modulation frequencies. Since small dimensions were used and the light emission processes are impact ionization and avalanche related, very high modulation frequencies could potentially be achieved. The current results as in Fig. 5(b) indicated that potential optical coupling could be achieved in these structures of up to 30 GHz.

In the third test structure (TS3), as in Fig. 2(c), a vertical cubical columnar structure was used for both the optical source as well as for the detector structure. The Si-Ge pn region was biased into reverse bias, and hence the Si Ge junction formed an avalanching light emitting source. The design motivation for this structure was indeed, that Si-Ge detector structure as elucidated in Figs. 2(a)–2(c), itself had a realized transition frequency of up to 80 GHz, it can be assumed that the reverse bias base–collector junction, when placed in avalanche reverse bias mode could attain similar modulation frequencies. The optical waveguide was similar as in TS2 but the silicon nitride layer lateral thickness was strategically reduced in lateral width dimension as shown in Fig. 1(c). The reduced waveguide core would enable less modal dispersion in the waveguide and boost single mode throughput at higher frequencies.[30,31]

A similar trend for optical coupling was observed as in Fig. 5(b). Mid frequencies S21 coupling reached a peak at −50 dB coupling at about 600 MHz and then reduced to lower values with increase in frequency. A much higher difference is observed between the forward transmission scattering S21 than for the reverse scattering parameter S12. The coupling magnitude for S21 is about the same as for the TS2 structure. However, the S12 reverse scattering is seemingly much less at −80 dB at 100 MHz. This indeed indicates less parasitic coupling in the structure at lower frequencies. This observed behavior is attributed to the pillar-like vertical and stacked nature of the optical source and the detector, which increased capacitances to the ground plane, as seen at the input and the output terminal in this specific structure, and which then also enabled a parasitic resistive and capacitive path along the substrate between the source pillar stricture and the detector pillar structure. Since normal pn junctions were used, some depletion layer capacitances existed along the substrate path. These capacitances are seemingly much higher than for the Schottky contact depletion layer as in structure TS2, and this is presumably responsible for the reduction in throughput at frequencies higher than 600 MHz. The increase in parasitic

coupling above 3 GHz probably originates from this path. Particularly, the bias voltage at the detector using a substrate embedded conduction channel could increase the parasitic coupling through the substrate. Weak alignment between the optical source point and the waveguide core could also be a serious limitation in this structure, especially since the waveguide core structure is much reduces as compared to the waveguide used in TS2, which would reduce the coupling factor drastically. The increased coupling and reduced parasitic coupling that occurs at the lower frequencies could be considered as important assets of this structure.

5 Potential Applications of the Optical Link Structures

Wada et al. proposed a H-shape configuration waveguide and 0.35-μm wavelength technology system for clock pulsing of CMOS subsystems. The waveguide technology and optical link structures as described in this paper could substantially augment and add a new dimension to this proposal. It particularly proposes the realization of on chip optical sources. Key constituents of such a system are an effective silicon IC compatible optical source, compatible optical wave guiding, effective optical coupling to the waveguide, and optical columniation circuitry, which all seems to be highly viable from the present analyses and proposed technology designs as developed in this study. Particularly, the cost of production of optical signal processing on silicon chip may offer various competitive options.

The realization of diverse other silicon IC or silicon CMOS-based microphotonic systems as well as the incorporation of a whole range of new on-chip microsensors into silicon IC technology are also most viable with this technology. Particularly, for next generation, micro-optoelectro-mechanical systems (MOEMS) sensors, lab-on-chip technologies, as well as in biomedical microsensor applications. In most cases, it merely implies a transfer of technology as developed in other systems to the silicon RF circuitry and Si-Ge waveguide technology. The advantages are achieving high levels of miniaturization, higher reliability levels, a vast reduction in technology complexity, and a drastic reduction in cost of producing associated systems. We have made some definite proposals in this regard through provisional patenting and IP protection.[41–44]

A particular further system that is proposed is a microfluidic type of microphotonic system design such that light is transmitted from integrated waveguide elements through a recess cavity in the silicon platform, The transmitted light interacts with an integrated detector and waveguide elements on the opposite side of the recess structure. In this module, optical light is focused by transmitting refractor lenses such that the transmitted light is detected by a single detector element or an array of optical detector elements. Figures 6(a) and 6(b), schematically, present the components of such a system. If a fluidic flow of gas or liquid or particles is transferred in the optical path's way in the recess cavity, the optically detected signal will be modulated and information of the gas or fluid can be extracted and analyzed. These could involve absorption analyses, or rate of absorption change, absorption pulsation or even spectroscopic analyses of transmitted or reflected light by a series of silicon detectors. Such a sensor system can reveal content about the material composition, the constituents, and even flow rate and other physical parameters as associated with the fluid.

6 Main Conclusions as Derived from This Study

The following main conclusions can be derived from the work as presented in this paper.

1. The designs and first iteration results as demonstrated in this work indeed indicate that the utilization of Si AMLEDS, TEOS, and Si-N-based waveguides, and employing the columnar processing capability as offered by the SiGe RF bipolar process, indeed offer good potential for realizing optical coupling over link distances up to 50 μm, to well into the GHz in silicon mainstream technology in the future at low economic cost figures.
2. The utilization of Si-Ge detector technology and the utilization of Si-Ge detector structure in the current commercial 0.35 RF bipolar process with its superior high RF frequency operation together with the high modulation characteristics of Si AMLEDs particularly show good potential.

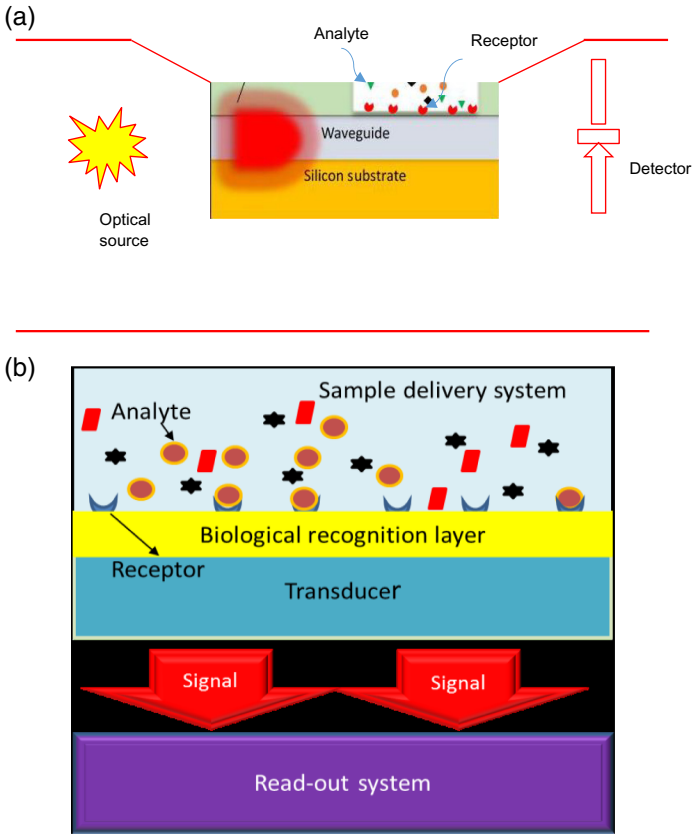

Fig. 6 Schematic representation of a futuristic on-silicon-chip bio-sensor type transducer with the four basic parts. (a) Schematic representation of a proposed on-silicon-chip waveguide-based-biosensor showing a recess in the outer chip layers with a receptor layer binding preferentially with a targeted analyte, changing the optical properties of the waveguide, and a difference then being detected by a silicon detector. (b) More detail of the biointeraction process and possible signal processing further illustrating how biochemistry is combined with electrochemistry and electro-optics to uniquely identify an analyte gas, a biogas, or a biofluidic sample.

3. The utilization of specific custom designed structures shows that compromises can be achieved between optical link losses and attainable throughput frequencies to well into the GHz range. Particularly, the low capacitance Schottky contact and wider silicon nitride core waveguide as tested and analyzed in this work show attainable coupling at −35 dB at throughput frequencies up to, potentially, 30 GHz. These results indicate potential digital modulation at these frequencies and compare extremely favorable with latest results obtained by Dutta et al. and Argawal et al., with their proved clear digital modulation of frequencies of up to 2 Mbps at a few nJ/bit.[23]
4. The optical coupling as demonstrated in this work was also achieved through waveguiding structures over distances of up to 50 μm, while previous work demonstrated tarted mere optical coupling through the adjacently lying structures in the silicon substrate, which can also be regarded as an advancement in technology achievement.
5. Further important derivation from this work is that alignment of optical sources to the waveguide cores in the integrated circuit optical link structures, the elimination of parasitic coupling paths to the ground through the Si Ge HBT pillar structures, lateral coupling in the silicon substrate, and placing of DC voltage bias points in the structures, are all identified limitations in the current designed structures. The authors are, however, convinced that most of these can be eliminated and improved upon in subsequent more careful and dedicated designs
6. The silicon-based waveguide technology as demonstrated, together with the choice of 0.75 μm operating wavelength, may show new routes of development and applications

for the field of silicon photonics in future, and the application of Si AMLEDs, may also indicate an important spin-off technology toward low-cost and ease of fabrication routes in future, enabling ease of integration with well-established silicon integrated circuit technology, with all its processing and memory interaction opportunities.

7. The current technology as utilized in this work is also very near to standard Si CMOS processing technology features, and incorporation and migration of this technology into CMOS technologies are hence greatly viable.

Acknowledgments

The test structure as demonstrated was realized in association with Université Paris Est, ESYCOM, ESIEE Paris, France. The utilization of advanced RF characterization facilities at this institution was therefore gratefully acknowledged. Dr. Zerihun Tegnegne and Carlos Viana from ESIEE would like to also thoroughly thank for their assistance with the RF characterization as demonstrated in this work. The content in this article forms the subject of recent PCT Patent Application PCT/ZA2010/00032 of June 2010, "An all-silicon 750 nm (submicron) CMOS and SOI-based optical communication system," PCT Patent Application PCT/ZA2010/00033 of June 2010 "MOEMS sensor device" (Several priority patents); PCT Patent Application PCT/ZA2010/00031 of June 2010, "Wavelength specific Si LED light emitting structures and arrays," and "650 nm Silicon Avalanche Light Emitting Diode," PCT/ZA2017/050052, University of South Africa in 2018.[41–44] These all deal with our latest technology definitions about Si Av LED CMOS-based optical communication systems, Si Av LED design, CMOS waveguide design, CMOS modulator, and switch design, CMOS-based data transfer systems, CMOS microphotonic system, and Micro-Opto-Electro-Mechanical Systems sensors design. All the patents as listed are currently assigned to Tshwane University of Technology and the University of South Africa. Collaboration and commercialization of the developed technologies are encouraged by interested third parties. The funders had no role in the design of the study; in the collection, analyses, or interpretation of data; in the writing of the manuscript, or in the decision to publish the results. This research received external funding from the South African National Research Foundation (Grant No. FA200604110043), NRF KIC (Grant No. UID 87297) and SANRF travel block grants. This work was also partly supported by the French government in the framework of the FUI8 ORIGIN project (Optical-Radio Infrastructure for Gigabit/s Indoor Networks). The study was conducted according to the guidelines of the declaration of Helsinki of the local college Institutional Review Board and Ethics Committee of University of South Africa.

References

1. J. A. Kubby and G. Reed, "Introductory remarks. Silicon photonics V," *Proc. SPIE* **6477**, ii–iii (2010).
2. C. Scow, F. Doany, and J. Kash, "Get on the optical bus," IEEE Spectrum http://spectrum.ieee.org/semiconductors/optoelectronics/get-on-thebus (2010).
3. E. A. Fitzgerald and L. C. Kimerling, "Silicon-based technology for integrated optoelectronics," *MRS Bull.* **23**(4), 39–47 (1998).
4. R. Soref, "Applications of silicon-based optoelectronics," *MRS Bull.* **23**(4), 20–24 (1998).
5. N. Savage, "Linking with light," *IEEE Spectrum* **39**(8), 32–36 (2002).
6. K. Wada, "Electronics and photonics convergence on silicon CMOS platforms," *Proc. SPIE* **5357**(16), 53–57 (2004).
7. W. G. Gynoweth and K. G. McKay, "Photon emission from avalanche breakdown in silicon," *Phys. Rev.* **102**, 369–376 (1956).
8. K. D. Hirschman et al., "Silicon-based visible light-emitting devices integrated into microelectronic circuits," *Nature* **384**, 338–341 (1996).
9. J. C. Brummer, H. Aharoni, and M. du Plessis, "Visible light from guard ring avalanche silicon photodiodes at different current levels," *South Afr. J. Phys.* **16**(1/2), 149–152 (1993).
10. H. Aharoni and M. Du Plessis, "The spatial distribution of light from silicon LED's," *Sens. Actuators A* **57**(3), 233–237 (1993).

11. P. M. Fauchet, "Progress toward nano-scale silicon light emitters," *IEEE J. Sel. Top. Quantum Electron.* **4**, 1020–1028 (1998).
12. M. A. Green et al., "Efficient silicon light-emitting diodes," *Nature* **412**, 805–808 (2001).
13. J. Kramer et al., "Industrial CMOS technology for the integration of optical metrology systems," *Sens. Actuators A* **A37–38**, 527–533 (1993).
14. L. W. Snyman, H. Aharoni, and M. Du Plessis, "Two order increase in the quantum efficiency of silicon CMOS n+pn avalanche-based light emitting devices as a function of current density," *IEEE Photonics Technol. Lett.* **17**, 2041–2043 (2005).
15. L. W. Snyman, M. Du Plessis, and H. Aharoni, "Injection-avalanche based n+pn Si CMOS LED's (450–750 nm) with two-order increase in light emission intensity—applications for next generation silicon-based optoelectronics," *Jpn. J. Appl. Phys.* **46**(4S), 2474–2480 (2007).
16. H. C. Lee and C. K. Liu, "Si-based current-density-enhanced light emission and low-operating-voltage light-emitting/receiving designs," *Solid-State Electron.* **49**(7), 1172–1178 (2005).
17. L. W. Snyman et al., "Optical sources, integrated optical detectors, and optical waveguides in standard silicon CMOS integrated circuitry," *Proc. SPIE* **3953**, 20–36 (2000).
18. M. Beals et al., "Process flow innovations for photonic device integration in CMOS," *Proc. SPIE* **6898**, 689804 (2008).
19. G. Gunn et al., "A 40-Gbps CMOS photonics tranceiver," *Proc. SPIE* **6477**, 64770N (2007).
20. R. K. Schneider and H. Zimmerman, "Highly sensitive optical receivers," in *High Performance Electron Devices for Microwave and Opto-electronic Applications*, A. Rezazadeh, Ed., Springer, New York (2006).
21. K. Xu, H. Liu, and Z. Zhang, "Gate-controlled diode structure based electro-optical interfaces in standard silicon-CMOS integrated circuitry," *Appl. Opt.* **54**(21), 6420 (2015).
22. S. Dutta et al., "Monolithic optical link in silicon-on-insulator CMOS technology," *Opt. Express* **25**(5), 5440–5456 (2017).
23. V. Agarwal et al., "Optocoupling in CMOS," in *IEEE Int. Electron Devices Meeting (IEDM)*, pp. 32.1.1–32.1.4 (2018).
24. D. Rosales et al., "Full area emitter Si-Ge phototransistor for opto-microwave circuit applications," in *9th IEEE Int. Conf. on Group IV Photonics, GFP* (2012).
25. J.-L. Polleux et al., "An heterojunction SiGe/Si phototransistor for opto-microwave applications: modelling and first experimental results," in *GAAS Conf. of the Eur. Microwave Week 2003*, Munich, pp. 231–234 (2003).
26. L. W. Snyman, K. A. Ogudo, and D. Foty, "Development of a 0.75 micron wavelength, all-silicon, CMOS-based optical communication system," *Proc. SPIE* **7943**, 79430K (2011).
27. K. A. Ogudo et al., "Optical propagation and refraction in silicon complementary metal-oxide-semiconductor structures at 750 nm: toward on chip optical links and micro-photonic systems," *J. Micro Nano-lithogr. MEMS MOEMS* **12**(1), 013015 (2013).
28. K. A. Ogudo et al., "Towards 10–40 GHz on-chip micro-optical links with all integrated Si Av LED optical sources, Si N based waveguides and Si-Ge detector technology," *Proc. SPIE* **8991**, 899108 (2014).
29. L. W. Snyman et al., "Increased efficiency of silicon light-emitting diodes in a standard 1.2-μm silicon complementary metal oxide semiconductor technology," *Opt. Eng.* **37**(7), 2133–2141 (1998).
30. L. W. Snyman, K. Xu, and J.-L. Polleux, "Micron and nano-dimensioned silicon LEDs emitting at 650 and 750–850 nm wavelengths in standard Si integrated circuitry," *IEEE J. Quantum Electron.* **56**(4), 1–10 (2020).
31. L. W. Snyman et al., "Stimulation of 700-900 nm wavelength optical emission from Si AMLEDs and coupling into Si_3N_4 waveguides using a RF silicon integrated circuit process," *OSA Continuum (USA)* **3**(4), 798–813 (2020).
32. L. W. Snyman et al., "Higher intensity SiAvLEDs in an RF bipolar process through carrier energy and carrier momentum engineering," *IEEE J. Quantum Electron.* **51**(7), 3200110–3200125 (2015).
33. J. M. Senior, *Optical Fiber Communications, Principles and Practice*, 3rd ed., Prentice Hall, Upper Saddle River, New Jersey, pp. 456–465 (2008).

34. H. Zimmermann, "Improved CMOS-integrated photodiodes and their application in OEICs," in *Proc. IEEE 1997 Workshop on High Perform. Electron Devices for Microwave and Opto-Electron. Appl.*, King's College, London, pp. 346–351 (1997).
35. K. Schneider and H. Zimmerman, *Highly Sensitive Optical Receivers*, Springer, Berlin (2006).
36. L. W. Snyman, K. Xu, and J.-L. Polleux, "Micron and nano-dimensioned Silicon LEDs emitting at 650 and 750–850 nm wavelengths in standard Si integrated circuitry," *IEEE J. Quantum Electron.* **56**(4), 1–10 (2020).
37. M. D. Rosales, J-L. Polleux, and C. Algani, "Design and implementation of SiGe HPTs using an 80-GHz SiGe bipolar process technology," in *IEEE 8th Int. Conf. on Group IV Photonics (GFP)*, pp. 243–245 (2011).
38. A. Chatterjee, B. Bhuva, and R. Schrimpf, "High-speed light modulation in avalanche breakdown mode for Si diodes," *IEEE Electron Device Lett.* **25**(9), 628–630 (2004).
39. L. W. Snyman et al., "Stimulating 600–650 nm wavelength optical emission in monolithically integrated silicon LEDs through controlled injection-avalanche and carrier density balancing technology," *IEEE J. Quantum Electron.* **53**(5), 1–9 (2017).
40. A. Gorin et al., "Fabrication of silicon nitride waveguides for visible-light using PECVD: a study of the effect of plasma frequency on optical properties," *Opt. Express* **16**(18), 13509 (2008).
41. L. W. Snyman and D. Foty, "An all-silicon 750 nm (sub-micron) CMOS and SOI-based optical communication system," PCT Patent Application PCT/ZA2010/00032 of (Priority patents: ZA2010/00200, ZA2009/09015, ZA2009/08833, ZA2009/04508) (2010).
42. L. W. Snyman, "MOEMS sensor device," PCT Patent Application PCT/ZA2010/00033 (2010).
43. L. W. Snyman, "650 nm Silicon avalanche light emitting diode," PCT Patent Application WO /2018/049434, PCT/ZA2017/050052, University of South Africa (2018).
44. L. W. Snyman, "Wavelength specific Si LED light emitting structures and arrays," PCT Patent Application PCT/ZA2010/00031 (2018).

Lukas W. Snyman received his PhD in semiconductor physics from the University of Port Elizabeth, South Africa, in 1987. He is currently a research and innovation professor at the College for Science Engineering and Technology, University of South Africa, Florida, Johannesburg. He has published about 120 scientific articles, mostly in international conference proceedings and scientific journals. He is also author and co-author of three scholarly chapters in *Intech* books. The latest was on "Integrating Micro-Photonic Systems and MOEMS into Standard Silicon CMOS Integrated Circuitry." He is the main inventor of five granted USA, co-inventor of two granted USA patents, main inventor of two European patents, two Korean patents, one Chinese patent, and eleven granted SA patents. He was nominated for the National Science Technology Forum award in the International Year of Light in South Africa, in 2017. He recently received an academic excellence award of the Most Prolific Innovator of the University of South Africa more than a period of 5 years in 2020. He is a current member of the Institute for Electrical and Electronic Engineers in the USA and a member of the Society for Photonic and Instrumentation Engineers in the USA. He was the main project manager and a device designer of this research study in association with Prof. Polleux at the Université Paris Est., ESYCOM, ESIEE, Paris, France and a PhD student Kingsley Ogudo.

Kingsley A. Ogudo received his N.Dip, NHD, BTech, and MTech degrees, all in electrical and electronics engineering, from Federal Polytechnic, Nigeria and the Tshwane University of Technology, South Africa, in 1998 to 2010. Since 2015, he has been a senior lecturer and a researcher in the Department of Electrical Engineering at the University of Johannesburg. He did his PhD study at the Université Paris Est., ESYCOM, ESIEE, Paris, France with the title "Development of edge-emitting Si/SiGe-based optical sources operating in the visible and near-visible range wavelength for sensing and communication applications" under the supervision of Prof. Polleux, Prof. Snyman, and Prof. Billabert. His research interest includes electronic, optoelectronic devices, telecommunication engineering high-frequency electronics, physics, and mathematics. He was mainly responsible for the DC and AC characterization in this work using a HP model 8510 (50 MHz to 40 GHz) Network Analyzer system with Prof. Polleux and Prof. Snyman.

Zerihun G. Tegnege received his bachelor of science degree in electrical engineering from Arbamich University, Ethiopia, in 2007, his master's degree in optical communications and photonic technologies from Polytechnic di Torino, Italy, in 2012, and his doctoral degree from the Université Paris-Est, France, in electronics, optoelectronics, and systems. He was a postdoctoral researcher at XLIM Research Institute in France. He is currently a researcher at ESYCOM Laboratory within ESIEE, Paris. His research interest includes the study of integrated photonics, optoelectronic and microwave photonics, radio-over-fiber systems, and photonics radar imaging systems. In this work, he mainly assisted Dr. Ogudo on the network analyses of the optical links with the HP model 8510 (50 MHz to 40 GHz) network analyzer system with Prof. Polleux and Prof. Snyman.

Jean-Luc Polleux received his degree/Diplôme d' Ingénieur in microelectronic from ENSEIRB, Bordeaux, France, his DEA degree in electronic and telecommunications from the University of Bordeaux, France, both in 1997, and his PhD in the optomicrowave field from CNAM, Paris, in 2001. He is currently an associate professor at ESYCOM Lab, Université Gustave Eiffel, CNRS UMR 9007, Noisy Le Grand, France. His current interest involves microwave-photonics devices and systems for radio-over-fiber applications with special emphasis on microwave phototransistors (SiGe/Si and InGaAs/InP), silicon-based integration and packaging, analogue VCSELs, and optomicrowave devices modeling. He published more than 60 scientific publications and 2 patents. He is an administrator of Optics Valley, Ile-de-France region and a head of ESIEE Paris as well as UPE's international master of electronics. He co-organized three international workshops and co-chaired the French microwave conference JNM2013. He was a guest editor of the *International Journal of Microwave and Wireless Technologies* in February 2014. He was responsible for the design and the implementation of the detector part of this study and managed also the AC characterization part of the study.

Anne-Laure Billabert received her engineering degree in electronics from IRESTE, University of Nantes, France, her DEA degree in electronic and radar from the University of Nantes, France, both in 1995, and her PhD in radar polarimetry field in 1999 from the University of Nantes, France. Since 1999, she has joined the ES-YCOM Laboratory and Cnam, Paris, France, as an associated professor. Her current research is centered in the topics of optomicrowave, mainly the simulation of optomicrowave link. She received the habilitation (HdR) in 2014 in the photonic-microwave field. From 2008 to 2018, she was in charge of the French Photonic-Microwave Club of the Société Française d' Optique. She acted as a co-supervisor for the PhD studies of Dr. Ogudo.

Herzl Aharoni is a professor emeritus in the ECE Department, Ben-Gurion University, Beer-Sheva, Israel. He encountered with light emission from silicon pn junctions (reported in 1955) during his doctoral research. Identifying its potential for practical utilization, he transformed this science into technology by association with M. Du Plessis and L. W. Snyman from Pretoria University, South Africa, as a team, designing, fabricating, and characterizing silicon light emitting devices (SiLEDs) that did not existed before, facilitating the fabrication of all-silicon integrated monolithic optoelectronic systems. His pioneering work in various fields of semiconductor physics was recognized by leading scientific societies, which granted him fellowship for his SiLEDs achievements: The American Physical Society, 2007; the International Society for Optical Engineering, 2011; the Optical Society of America, 2016; and the European Physical Society, 2018. He motivated the publication of this specific article and wrote the introduction section of the article. He was a main advocator for the application of Si AMLEDs in various applications since the early nineties and was an important mentor in this study during the initiation phases of the study.